

## Footprints in Sand: The Response of a Granular Material to Local Perturbations

Junfei Geng, D. Howell, E. Longhi, and R. P. Behringer

*Department of Physics and Center for Nonlinear and Complex Systems, Duke University,  
Durham, North Carolina 27708-0305*

G. Reydellet, L. Vanel, and E. Clément

*Université Pierre et Marie Curie, Paris 75231, France*

S. Luding

*ICA1, University of Stuttgart, Pfaffenwaldring 27, 70569 Stuttgart, Germany*

(Received 7 December 2000; published 2 July 2001)

We experimentally determine ensemble-averaged responses of granular packings to point forces, and we compare these results to recent models for force propagation in a granular material. We use 2D granular arrays consisting of photoelastic particles: either disks or pentagons, thus spanning the range from ordered to disordered packings. A key finding is that spatial ordering of the particles is a key factor in the force response. Ordered packings have a propagative component that does not occur in disordered packings.

DOI: 10.1103/PhysRevLett.87.035506

PACS numbers: 47.20.-k

Granular systems have captured much recent interest due to their rich phenomenology and important applications [1]. Even in the absence of strong spatial disorder of the grains, static arrays show inhomogeneous spatial stress profiles called stress (or force) chains [2]. Forces are carried primarily by a tenuous network that is a fraction of the total number of grains.

A fundamental unresolved issue concerns how granular materials respond to applied forces, and there are several substantially different models. A broad group of conventional continuum models (e.g., elastoplastic, etc.) posit an elastic response for material up to the point of plastic deformation [3]. The stresses in portions of such a system below plastic yield have an elastic response and satisfy an elliptic partial differential equation (PDE); those parts that are plastically deforming satisfy a hyperbolic PDE. Several fundamentally different models have recently been proposed. The  $q$  model of Coppersmith *et al.* [4] assumes a regular lattice of grains, and randomness is introduced at the contacts. This model successfully predicts the distribution of forces in the large force limit, as verified by several static and quasistatic experiments and models [4–6]. In the continuum limit, this model reduces to the diffusion equation, since the forces effectively propagate by a random walk. Another model [the oriented stress linearity (OSL) model] of Bouchaud *et al.* [7] has a constitutive law, justified through a microscopic model, of the form  $\sigma_{zz} = \mu\sigma_{xz} + \eta\sigma_{xx}$  (in 2D) in order to close the stress balance conditions  $\partial\sigma_{ij}/\partial x_j = \rho g_i$ . This leads to wave-like hyperbolic PDEs describing the spatial variation of stresses. In later work, these authors considered weak randomness in the lattice [8], and proposed a convection-diffusion (C-D) equation. A model proposed by Kenkre *et al.* [9] combines pure wave propagation and diffusion in the telegraph equation. Recently, Luding

*et al.* [10] and Bouchaud *et al.* [11] have proposed models that account for force fluctuations on both the length scale of grains and on the length scale of stress chains.

The range of predictions among the models is perhaps best appreciated by noting that the different pictures predict qualitatively different PDEs for the variation of stresses within a sample: e.g., for elastoplastic models an elliptic or hyperbolic PDE; for the  $q$  model, a parabolic PDE; and for the OSL model without randomness, a hyperbolic PDE. The impact of equation type extends to the boundary conditions needed to determine a solution: e.g., hyperbolic equations require less boundary information than elliptic equations. The importance of resolving which of these models applies under what circumstances was recently emphasized by de Gennes [12].

Here we explore these issues through experiments on a 2D granular system consisting of photoelastic (i.e., birefringent under strain) polymer particles [6] that are either disks or pentagons. By viewing the particles through an arrangement of circular polarizers (a polariscope) it is possible to characterize the stress on the particles [6]. We record polariscope images with a digital camera that has a resolution of 0.045 cm per pixel, whereas the typical particle is slightly less than 1 cm. Near a contact, the stresses within a particle are very nonuniform, and lead to a series of light and dark bands in the polariscope image intensity,  $I$ , with the density of bands increasing monotonically with the force at the contact. We exploit this fact to produce a force calibration in terms of  $G^2 \equiv |\nabla I|^2$ , where we compute  $G^2$  as a function of position at the pixel scale.  $G^2$  is sensitive to the density of bands, and hence to the local contact force. We obtained a calibration of  $G^2$  vs mean force on a disk by three mutually consistent ways: (1) by applying known forces to the boundary of a small number of particles and at the same time measuring  $\langle G^2 \rangle$ , (2) by

applying various uniform loads to the upper surface of a large rectangular sample (width larger than height to avoid the Janssen effect), and (3) by measuring the hydrostatic force vs depth,  $z$ . The inset of Fig. 1 shows results for the second technique. The body of Fig. 1 shows examples of the third technique for two different samples, as well as the calculated profiles for the hydrostatic pressure,  $\rho g z$  (lines) using the known densities,  $\rho$ . Note that there are no free parameters for these lines. These calibrations are effective until the forces are so large that it is no longer possible to resolve the bands clearly, a condition that does not occur in these studies.

We used two different particle types, disks and pentagons, in order to construct packings of varying degrees of spatial order or disorder. For monodisperse disks, we obtained a highly ordered packing. With bidisperse distributions, we modified the disorder in a controlled way [13] characterized by the parameter  $\mathcal{A} = \langle a \rangle^2 / \langle a^2 \rangle$ . The brackets refer to averages over the sample for powers of the disk diameters  $a$ . To vary  $\mathcal{A}$ , we used mixtures of two disk diameters:  $a_1 \approx 0.7$  cm and  $a_2 \approx 0.9$  cm. Both types of disks had a thickness of 0.64 cm. The pentagons had the same thickness as the disks, and a side length of 0.7 cm. A sample, typically  $\sim 60$  particles wide and 25 particles high, was placed in a nearly vertical plane. To keep the sample from collapsing, it rested against a smooth powder-lubricated glass plate that was inclined from the vertical by a small angle,  $\leq 3^\circ$ , hence minimizing the friction with the plate. The sample rested on a rigid metal base, and was confined at the sides by rigid metal bars. The samples were prepared by gently adding particles to the upper surface until the full amount of particles was in place.

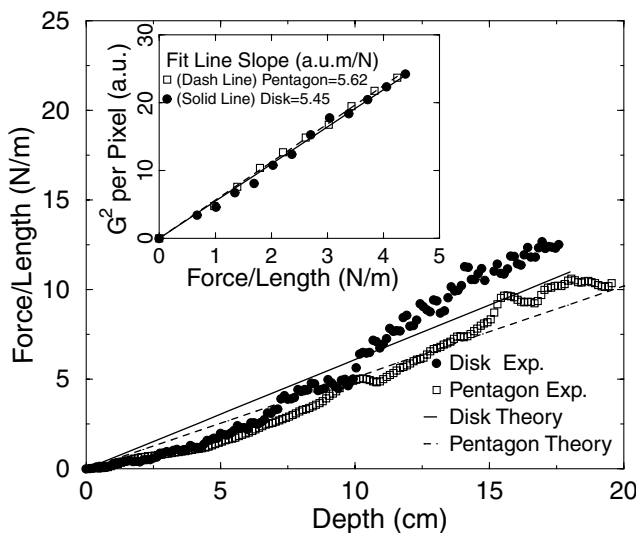


FIG. 1. Hydrostatic pressure due to gravitational force alone versus depth determined from  $G^2$ . The expected slopes of the stress-height curves are calculated from the known packing fraction ( $\gamma = 0.91$  for disks;  $\gamma \approx 0.75$  for pentagons). Inset shows the multiparticle  $G^2$  calibration by applying known loads to the upper surface of the layer.

Figure 2a shows a typical raw polariscope image ( $I$ ) in the absence of any applied force, besides gravity. In this image and the image shown in Fig. 2b, bright regions correspond to large forces, and are the stress chains noted above. The stress at the bottom of the sample is larger than at the top due to gravitational head, and the mean stress was a linearly increasing function of depth.

We measured the system point-force response by placing a known weight carefully on top of one particle in the approximate center of the sample, producing a local vertical force (Fig. 2b). We then removed the weight. For the monodisperse and pentagonal packings described below, we used only responses where the particles remained undisturbed by this process. For polydisperse disk samples, some small rearrangement of the surface grains always occurred, however. For each realization, we computed the square gradient,  $G^2$ , at the pixel scale, and obtained the stress difference between successive images of  $G^2$  (Figs. 2c and 2d), containing only the response from the point perturbation, with the linear hydrostatic head effects removed. We refer to this difference as  $\Delta G^2$ .

We repeated this process for many different rearrangements of the particles, typically 50 times for each set of particles. The images of Figs. 2c and 2d show that the responses for  $\Delta G^2$  are complicated and differ significantly from realization to realization. There are at least two approaches to address the large variability among realizations: (1) Obtain information on an ensemble of realizations; or (2) perturb the system over a larger number of grains in order to obtain a larger-scale averaging. Here we pursue the first option. Below, we compare these average responses to continuum models which do not generally

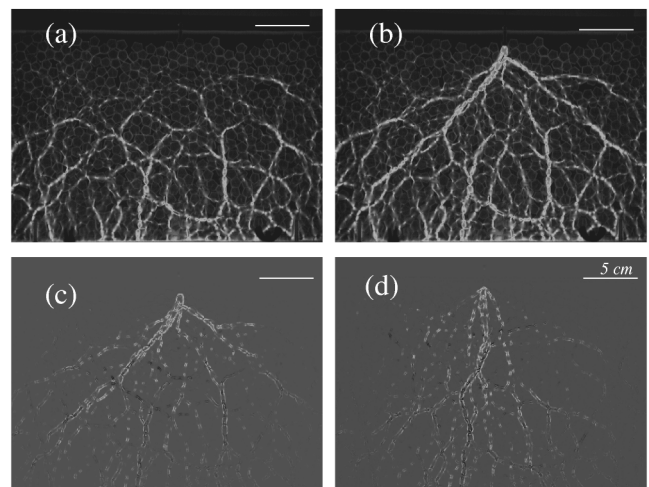


FIG. 2. Images for pentagons showing (a) the force pattern due to hydrostatic head. (b) The combined response to gravity and a point source. (c) The response to a point force,  $\Delta G^2$ , obtained by subtracting the  $G^2$  version of (a) from (b). (d) Similar to (c), but with a different grain configuration. The bars correspond to the length scale of 5 cm. Note that the images do not extend to the side boundaries. Parts (a) and (b) are images of intensity,  $I$ , and parts (c) and (d) are images of  $\Delta G^2$ .

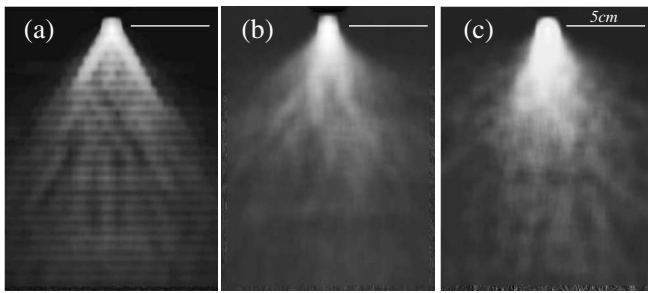


FIG. 3. Mean response from  $\Delta G^2$  for 50 trials of a 50 g point force for (a) a uniform hexagonal packing of disks, (b) a bimodal packing of disks with  $\mathcal{A} = 0.99$ , and (c) pentagons. The size of each image is about  $18.0 \times 13.5 \text{ cm}^2$ . The bars correspond to a length of 5 cm.

contain any information on the particle size. However, the particle size is the smallest length scale for which such comparisons seem reasonable.

In Fig. 3, we show using grey scale the average response,  $\Delta G^2$ , for monodisperse disks, a mixture of disks, and pentagons, for a point load of 50 g. In Fig. 4, we show more quantitative data for the force response,  $\Delta G^2$ , along a series of horizontal lines at depths,  $z$  (measured from the top). These data show clear differences depending on the packing geometry. The monodisperse packing shows two peaks emerging from the central source, broadening with  $z$ , but remaining clearly identifiable. For the bidisperse packing, the peaks are also present, but much less sharply resolved. Data for the pentagons show no evidence for wave-like stress propagation. There is some noisy structure for the pentagon response at the greatest depths. We believe this is due to the fact that it is relatively difficult to rearrange the interlocked pentagonal packing at large depths; hence chains tended to appear there in nearly the same places. In any event, this effect occurs only deep in the pile.

A key question is then which model best describes these results. The answer clearly depends on the amount of spatial order in the packing. For the ordered (monodisperse) packing, the C-D model proposed by Claudin *et al.* [8] provides reasonable agreement with the data, as shown by the fit lines of Fig. 4. However, there are clear departures between the data and fits to the C-D model, since the central peak persists to depths for which the C-D model predicts no such feature, and the two side structures fall to the noise level for  $h > 8d$ . The recent models proposed by Luding *et al.* [10] and by Bouchaud *et al.* [11] predict the presence of the central feature, and thus offer improved fits (details to be discussed elsewhere).

For the disordered packings, best characterized by pentagons, the one central peak might be described by either diffusion or by elasticity. It is possible to distinguish which of these is best from the width,  $W(z)$ , of the response peak. For a diffusive model,  $W$  should grow as  $\sqrt{z}$ . For an elastic layer, the response to a point force is a modified

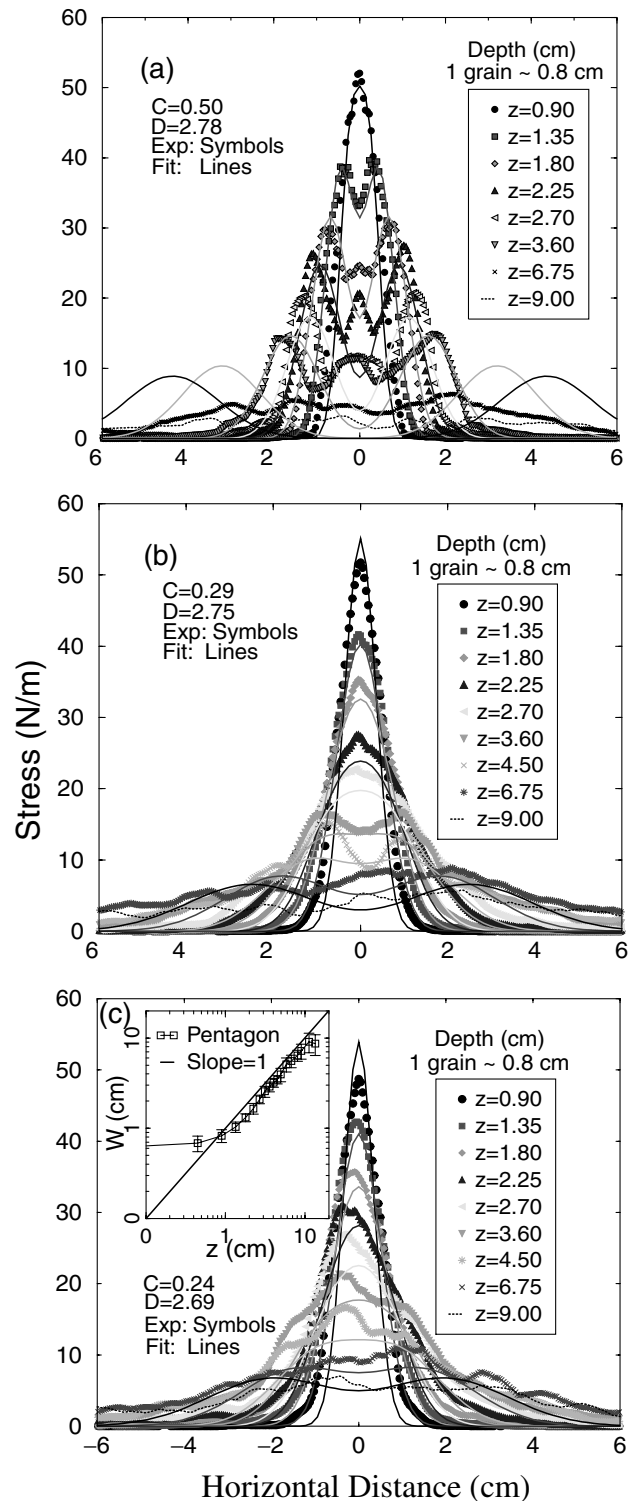


FIG. 4. Photoelastic response (force per length-stress in 2D) to a point force vs horizontal distance,  $x$ , at various depths,  $z$ , from the source. (a) For ordered disks, (b) for bimodal disks, and (c) for pentagons. Also shown are fits of the response to the convection-diffusion model. In all fits, the C-D model parameters are  $c$ , the dimensionless velocity and  $D$ , the diffusion coefficient in units of pixels (1 pixel = 0.45 mm). Inset part (c):  $W$  vs  $z$  for the response for pentagons.

Lorentzian with  $W \propto z$  for moderate  $z$ . We show in the inset of Fig. 4c data (on log scales) indicating that  $W \propto z$  over the experimental range when  $z > d$ , as in an elastic response.

The pentagon results, including the linear dependence of  $W$  on  $z$ , are consistent with recent experimental work by Reydellet *et al.* [14] for 3D disordered packings, with numerical simulations by Moreau [15], and with the recent theoretical work of Bouchaud *et al.* [11], who find a crossover to an elliptic response beyond a length scale controlled by the level of disorder. Recent experiments have also been carried out by Rajchenbach [16], who used cuboidal blocks of photoelastic material in a similar arrangement to that used here. These experiments showed a parabolic outer envelope of the response. Since it is difficult to know the nature of the intergrain contacts and the extent of their order or disorder, it is also difficult to place these measurements in the present context.

To conclude, we have measured the force response of 2D granular packings to local force perturbations. There are large variations for any given response, and we consider averages over many realizations. For packings with strong spatial order, the mean response has a strong propagative part, and convection-diffusion or more recent models [10,11] give a reasonable description. As the amount of disorder increases, the propagative component diminishes, and the response is most like that of an elastic material. Interestingly, the connection between order or disorder and the force response may provide a way to characterize the disorder in granular samples, something that may be important for understanding experiments where the amount of disorder of a packing was clearly important [17]. These results raise additional questions for future work such as the need to investigate the vector character of force propagation (e.g., forces applied at arbitrary angles to a surface, forces applied in the interior). Another important issue concerns the statistical variability that can be expected in a single realization.

We appreciate helpful interactions with P. Claudin, I. Goldhirsch, D. Schaeffer, and J. Socolar. The work of S. L. was supported by the Deutsche Forschungsgemeinschaft (DFG) and the National Science Foundation. The work of G. R., L. V., and E. C. was supported by PICS-CNRS No. 563. The work of J. G., D. H., E. L., and R. P. B. was supported by the U.S. National Science Foundation

under Grants No. DMR-9802602 and No. DMS-9803305, and by NASA under Grant No. NAG3-2372.

- 
- [1] For broad perspectives see Focus Issue on Granular Materials [Chaos **9**, 509–696 (1999)]; *Physics of Dry Granular Media*, edited by H. J. Herrmann, J.-P. Hovi, and S. Luding, NATO ASI Series, (Kluwer, Dordrecht, The Netherlands, 1977); *Powders and Grains 97*, edited by R. P. Behringer and J. T. Jenkins (Balkema, Rotterdam, The Netherlands, 1997); H. M. Jaeger, S. R. Nagel, and R. P. Behringer, *Rev. Mod. Phys.* **68**, 1259 (1996).
  - [2] S. Ouaguenouni and J.-N. Roux, *Europhys. Lett.* **39**, 117–122 (1997).
  - [3] D. M. Wood, *Soil Behaviour and Critical State Soil Mechanics* (Cambridge University Press, Cambridge, U.K., 1990); R. M. Nedderman, *Statics and Kinematics of Granular Materials* (Cambridge University Press, Cambridge, U.K., 1992).
  - [4] C.-h. Liu, S. R. Nagel, D. A. Schecter, S. N. Coppersmith, S. Majumdar, O. Narayan, and T. A. Witten, *Science* **269**, 513 (1995); S. N. Coppersmith, C.-h. Liu, S. Majumdar, O. Narayan, and T. A. Witten, *Phys. Rev. E* **53**, 4673 (1996).
  - [5] D. K. Mueth *et al.*, *Phys. Rev. E* **57**, 3164 (1998); B. J. Miller, C. O'Hern, and R. P. Behringer, *Phys. Rev. Lett.* **77**, 3110 (1996).
  - [6] D. Howell, R. P. Behringer, and C. Veje, *Phys. Rev. Lett.* **82**, 5241 (1999); C. Veje, D. Howell, and R. Behringer, *Phys. Rev. E* **59**, 739 (1999); *Chaos* **9**, 599 (1999).
  - [7] J.-P. Bouchaud, M. E. Cates, and P. Claudin, *J. Phys. I (France)* **5**, 639 (1995); J. P. Wittmer, M. E. Cates, and P. Claudin, *J. Phys. I (France)* **7**, 39 (1997).
  - [8] P. Claudin, J. P. Bouchaud, M. E. Cates, and J. P. Wittmer, *Phys. Rev. E* **57**, 4441 (1998).
  - [9] V. M. Kenkre, J. E. Scott, E. A. Pease, and A. J. Hurd, *Phys. Rev. E* **57**, 5841 (1998).
  - [10] S. Luding, J. Geng, and R. P. Behringer (to be published).
  - [11] J.-P. Bouchaud *et al.*, *Euro. Phys. J.* **E4**, 451 (2001).
  - [12] P.-G. de Gennes, *Rev. Mod. Phys.* **71**, 374 (1999).
  - [13] S. Luding and O. Strauß, in *Granular Gases*, edited by T. Pöschel and S. Luding (Springer-Verlag, Berlin, 2000).
  - [14] G. Reydellet and E. Clément, *Phys. Rev. Lett.* **86**, 3308 (2001).
  - [15] J. J. Moreau, *Colloque Physique et Mécanique des Milieux Granulaires* (in French), Acte des Journées Scientifiques du LCPC, Sept. 2000, pp. 199–204 (2000).
  - [16] J. Rajchenbach, *Nature (London)* **406**, 708 (2000).
  - [17] G. W. Baxter, R. P. Behringer, T. Fagert, and G. A. Johnson, *Phys. Rev. Lett.* **62**, 2825 (1989).